1

2

A 1D River Hydraulic Model for Operational Flood Forecasting in the Tidal Potomac: Evaluation for Freshwater, Tidal, and Wind Driven Events

5

6

H.S. Mashriqui*[1], J.S. Halgren[1,2], S.M. Reed[1]

[1]NOAA, National Weather Service, Office of Hydrologic Development, 1325 East-West Highway, Silver Spring, MD 20910, USA. [2]Riverside Technology, Inc.

10

11

12

13

14

15

16

17

18

19

20

21

22

*Corresponding author. Address: Hydrology Lab., Office of Hydrologic Development, W/OHD-12, NOAA's National Weather Service, 1325 East-West Highway, Silver Spring, MD, 20910, USA. E-mail address: hassan.mashriqui@noaa.gov (H.S. Mashriqui).

26

27

28

Abstract The National Oceanic and Atmospheric Administration (NOAA) is working

towards improving water forecasts in the river-estuary transition zone. One operationally viable

method is to extend one-dimensional (1D) hydraulic models downstream well into the tidal

estuarine environment. Recent advances in NOAA's National Weather Service (NWS)

operational software infrastructure have made this method easier to implement using the

Hydrologic Engineering Center River Analysis System (HEC-RAS). Here, we evaluated the

strengths and limitations of an unsteady HEC-RAS implementation for the tidal Potomac River.

We calibrated the HEC-RAS model for harmonic tides and major historic freshwater flood

events and validated the model on recent freshwater and storm surge events, focusing on water

level gauges near Washington, D.C. Root mean squared error for tide simulation at the

Washington Waterfront gauge was 0.05 m (0.16 ft) with a phase error of about 2 hours. For

historic flood events, simulated peak water level error varied from -0.40 m (-1.34 ft) to 0.40 m

(1.34 ft) with a mean absolute error of 0.25 m (0.82 ft) at the Wisconsin Avenue gauge. While

HEC-RAS shows considerable potential to improve upon an existing empirical forecast

technique for freshwater, tidal, and freshwater-tidal events, HEC-RAS did not adequately model

wind-driven events because it does not include an explicit wind forcing term.

Therefore, to further understand the influence of wind on Potomac water levels, we

developed both a SOBEK 1D model and a ADCIRC 2D model for Hurricane Isabel. With storm-

specific calibration, wind driven simulations from SOBEK and ADCIRC improved peak water

level simulation for Hurricane Isabel over HEC-RAS. HEC-RAS without wind forcing missed

the Hurricane Isabel peak at the Washington Waterfront by 0.66 m while SOBEK and ADCIRC

came within 0.08 and 0.01 m respectively. Interestingly, little improvement was seen over HEC-

RAS in prediction of peak time. While SOBEK results show that a wind term in a 1D hydraulic

52   model can account for observed high water levels, our simple wind reduction factor calibration

53   technique should be replaced by a more physically-based approach to achieve more robust

54   implementations in the future.

57

1 INTRODUCTION

1.1 Motivation

The National Oceanic and Atmospheric Administration's (NOAA's) vision for Coast, Estuary, River Information Services (CERIS) (NOAA 2009) includes providing enhanced water information in coastal areas, and identifies improved river-estuary-ocean model linkages as a key mechanism to achieve this goal. The CERIS vision covers a range of forecast services including flow, water level, current, water quality, and ecosystem health. In this paper, we focus on methods to improve water level forecasts in the river estuary transition zone.

NOAA's National Weather Service (NWS) uses hydrologic models and one-dimensional (1D) hydraulic routing models to forecast river flows and stages at over 4,000 locations in the United States. Through the National Ocean Service (NOS), NOAA also produces estuary and ocean forecasts of tides, storm surge, waves, and estuarine circulation for a variety of users. Despite extensive modeling by both NWS and NOS, various gaps exist in the forecast services, particularly for the riverine-estuarine transition zone where the water elevation can be substantially influenced both by freshwater flows as well as tides and other open ocean effects. Because of these multiple influences, complex modeling is necessary to fully understand and forecast the water behavior in the river-estuary transition zone.

The riverine hydraulic model described in this paper fills the long standing gap in operational model coverage shown in Fig. 1. Prior to this work, the NWS Middle Atlantic River Forecast Center (MARFC) ran dynamic hydrologic models on the Potomac River only as far as the Little Falls Pump station above Washington, D.C. The upstream-most forecast from the NOS Chesapeake Bay Operational Forecast System (CBOFS) (Lanerolle et al. 2009) (described

80   below) is downstream of the confluence of the Anacostia and Potomac rivers. This left a fifteen

81   kilometer (nine mile) gap where neither the NWS nor NOS operational forecast models provided

82   water level simulations. This gap area includes nationally significant areas such as the National

83   Mall, Parks and Georgetown's Washington Harbor, where local businesses need more accurate

84   flood forecasts to guide decisions on when and where to erect movable flood walls. While

85   MARFC forecasters have had utilized empirical guidance curves to forecast water levels at one

86   point along this stretch for many years (Wisconsin Avenue near Washington, D.C.), they desired

87   an automated, dynamic hydraulic model with continuous spatial coverage.

88   **1.2   Rationale for Using HEC-RAS to Forecast Water Level on the Lower Potomac River**

89   Historically, NWS one-dimensional (1D) hydraulic models have proven to be a viable

90   option for generating accurate water level forecasts in coastal rivers (Fread and Lewis 1985).

91   Working closely with the US Army Corps of Engineers (USACE), the NWS has recently added

92   the USACE's Hydrologic Engineering Center River Analysis System (HEC-RAS) (Brunner

93   2000) computational engines to the suite of modeling tools available for operational river

94   forecasting (Moreda et al. 2009). The unsteady module of the HEC-RAS 1D hydraulic model is

95   used for river forecasting and is accessible to NWS forecasters through the Community

96   Hydrologic Prediction System (CHPS) (Roe et al. 2010). NWS adoption of HEC-RAS has

97   stimulated renewed interest at River Forecast Centers (RFC) to implement hydraulic models for

98   operational forecasting, particularly in coastal rivers.

99   In addition to the tidal Potomac River, we are aware of four other new, coastal HEC-RAS

100   implementation projects in progress at RFCs: (1) the Colorado River, TX; (2) a joint model of

101   several rivers in the Houston, TX, metropolitan region; (3) the Pascagoula River, MS; and (4) the

102   Waccamaw River, SC. Implementing new HEC-RAS models in the transition zone is a relatively

103 simple and cost-effective method for RFCs to improve the accuracy of forecasts at existing

104 forecast points and to expand water level forecast services to new locations.

105   Several operational estuary-ocean models which produce water level and flow data are

106 candidate sources for downstream boundary conditions for operational HEC-RAS

107 implementations in the Chesapeake Bay and elsewhere in the United States, including the Sea,

108 Lake and Overland Surges from Hurricanes (SLOSH) (Jelesnianski et al. 1992), Extratropical

109 Surge (ETSurge) (Kim et al. 1996), and Extratropical Surge and Tide Operational Forecast

110 System (ESTOFS) (NOAA Coast Survey Development Lab (CSDL) 2011). Table 1 summarizes

111 the available operational estuary-ocean models considered for this research.

112   Beyond operational modeling, recent research focused specifically on the Chesapeake

113 Bay Region makes the lower Potomac River an excellent test bed for transition zone modeling

114 and model evaluation since we can compare operational model results to research model results.

115 Two modeling efforts of particular interest are enhancements to the CBOFS operational forecast

116 system (Lanerolle et al. 2009) and an implementation of the Eulerian Circulation (ELCIRC)

117 model (A. Zhang et al. 2010; Y. Zhang et al. 2004) as part of the Chesapeake Bay Inundation

118 Prediction System (CIPS) demonstration project (Cho 2009; Cho et al. 2011). The CBOFS

119 estuary model, based on the Regional Ocean Modeling System (ROMS) (Shchepetkin and

120 McWilliams 2005), was developed primarily to produce operational tide and current forecasts for

121 the navigational community and has recently been enhanced to include three-dimensional water

122 quality as part of the forecast output. The current CBOFS model grid extends close to the

123 Anacostia – Potomac confluence as shown in Fig. 1.

124   An alternative to using a 1D river hydraulic model to model the transition zone and

125 bridge forecast gaps is extending an estuary-ocean model farther upstream. Cho et al. (2011)

126   worked toward this capability, showing accurate water level forecasts for the Washington, D.C.

127   area from ELCIRC simulations for Hurricane Isabel event in 2003. The flexible mesh feature of

128   their model allows calculations to be efficiently extended into the riverine environment.

129   However, while the Cho et al. (2011) model has been tested under some freshwater flood

130   conditions, it has not been tested with or calibrated to extreme freshwater flood conditions such

131   as the Potomac River flood of 1936, when peak flow was about 13,450 cubic meter per second

132   (cms) (475,000 cubic feet per second (cfs)). Also, the Cho et al. (2011) model is only available in

133   demonstration mode at an academic institution and therefore less likely for immediate use in an

134   operational environment.

135   The low computational demands of 1D river models offer additional advantages for

136   operational use. Existing NWS RFC hardware can easily run and re-run 1D river models to

137   accommodate changing weather and water conditions in a matter of minutes on a workstation as

138   compared to hours on a super computer for complex 2D models. Forecasters have expressed a

139   preference to re-run HEC-RAS using different boundary conditions available in operations

140   (Table 1) and this option is easily configurable within CHPS. Ensemble forecast runs including

141   1D river hydraulic models are also feasible with existing hardware. More generally, riverine

142   models such as HEC-RAS provide advanced tools for modeling the impacts of bridges, locks and

143   gates and other river obstructions, which are generally not included in the currently operational

144   or research 2D/3D estuarine models. Despite the advantages of 1D models, operational HEC-

145   RAS implementations are limited due to the lack of a wind forcing term in the momentum

146   equation.

1.3   Objectives

This paper describes creation, calibration, and validation of a HEC-RAS unsteady state

model for forecasting water level in the river-estuary transition zone for the lower Potomac

River. Building a model for operational forecasting requires some different considerations than

the more common steady-state HEC-RAS applications for engineering design. Therefore, we

expect documenting this study to provide useful lessons learned for future operational

forecasting implementations. We evaluate the model performance over a wide range of

conditions relevant to the transition zone, including events where freshwater runoff, tides and

wind play an important role. We also compare the model performance to MARFC's empirical

guidance curves for the Wisconsin Avenue gauge.

To understand the significance of wind directly on the hydraulics of the transition zone in

the Potomac, we construct two other models covering the lower Potomac that include explicit

wind forcing and compare results to HEC-RAS results for Hurricane Isabel. The first wind

model is a 1D implementation of SOBEK (Deltares 2011) and the second is an implementation

of ADCIRC 2D (Westerink et al. 1992). We identify several practical issues to consider when

implementing wind forcing in an operational 1D model including availability and consistency of

observed and forecast wind fields and effectiveness of available approaches to spatially and

temporally translate wind forces onto the 1D model geometry.

2   METHODOLOGY

This section describes how the HEC-RAS, SOBEK1D and ADCIRC 2D models were

built or applied to explore the dynamic influences on water level in the transition zone. We first

provide detail on the HEC-RAS model calibrated and validated first for tidally dominated events,

169   then for freshwater events. Our results will help forecasters understand what range of accuracies

170   to expect when using this model.

171   We subsequently describe the SOBEK 1D and ADCIRC 2D model implementations and

172   associated modeling experiments designed to better understand the impacts of including a wind

173   forcing term in the hydraulic computations during simulations of the Hurricane Isabel event in

174   2003.

175   **2.1   Lower Potomac HEC-RAS Model**

176   The tidal Potomac River unsteady HEC-RAS model domain covers about 183.4 km (114

177   miles) of the main stem of the Potomac and contains 89 cross-sections beginning where the river

178   enters Washington, D.C. just below Little Falls and extending to the mouth of the Potomac at the

179   Chesapeake Bay near Lewisetta, Virginia (Fig. 2). This domain includes the NWS service gap

180   area of about fifteen kilometers (nine miles) from SW Washington, D.C. to near Little Falls.

181   About eleven kilometers (seven miles) of the Anacostia River comprising 15 cross-

182   sections are included in the model as a tributary to the Potomac River. Although a study by the

183   Maryland Department of the Environment (MDE - D.C. DE-NRA 2007) indicates that there are

184   tidal influences farther upstream in the Anacostia River, we did not have the necessary

185   bathymetry information to extend the model. Other minor tributaries and lateral flows are not

186   included in the model. These tributaries account for about 14% of the total drainage area above

187   Lewisetta; however, most of this additional tributary drainage is below our primary forecast

188   locations of interest near Washington, D.C.

189   Observed or synthetic inflow time series defined the upstream boundary conditions of the

190   different model scenarios, while the downstream boundary condition at Lewisetta was a water

191   level time series.

192   We developed the Potomac HEC-RAS model cross-section geometry based on both

193   bathymetry data provided by NOS Coast Survey Development Laboratory (CSDL) and a geo-

194   referenced HEC-RAS model of the Potomac River from Little Falls to the Anacostia-Potomac

195   confluence developed for the Federal Emergency Management Agency (FEMA) Region 3. The

196   FEMA cross sections were used unmodified and new HEC-RAS cross sections were developed

197   downstream of the FEMA model domain using NOS-CSDL data. Where necessary, the USGS

198   7.5-minute Digital Elevation Model (DEM) (nominally 30- by 30-m data spacing) was used to

199   determine the bank and flood plain elevations. The vertical datum for time series plots and cross

200   section elevations are in mean sea level (MSL). Where applicable, elevations were converted to

201   MSL. Greenwich Mean Time (GMT) is used as the reference time frame.

202   Both the Potomac and Anacostia Rivers are highly influenced by freshwater inflow and

203   storm tides, and either of these or combinations of both are the major causes of flooding along

204   the tidal Potomac and the Anacostia River at Washington, D.C. and the City of Alexandria,

205   Virginia (Cho 2009; FEMA 2010). In the vicinity of Washington, D.C., the variation in the

206   river's water surface elevation over a normal tidal cycle ranges from 0.9 m to 1.2 m (3 ft to 4 ft)

207   (mean sea level, MSL). As shown in Table 2, during flooding events, water levels at Wisconsin

208   Avenue have reached nearly to 5 meters above MSL (16 ft) and can be as high as 3.7 m (12 feet)

209   above mean sea level near Washington, D.C. (FEMA 2010). To attain predictive skill over the

210   wide range of possible conditions, we calibrated the HEC-RAS model to tidal forcings

211   representative of low flow conditions and then to historical record flood conditions. The

10

212   calibrated parameters were validated with recent low-flow periods as well as storm surge and

213   freshwater flood events.

214   *2.1.1   Calibration to Tidal Boundary with HEC-RAS*
215   Baseline calibration of the HEC-RAS Manning's n roughness parameters was performed

216   to evaluate the model's ability to reproduce harmonic constituents estimated by the NOAA's

217   Center for Operational Oceanographic Products and Services (CO-OPS). The harmonic

218   constituents are the amplitude and phase parameters of various cosine functions which when

219   added, give the total tidal variation at a particular coastal location independent of the effects of

220   wind, freshwater flows, and other deviations from the pure astronomical tide (Schureman 1941).

221   The tidal evaluation used 29 days of astronomical tide at Lewisetta (NOAA's CO-OPS Station

222   ID 8635750) as the downstream boundary condition. A minimal 0.3 cms (10 cfs) flow was used

223   for the upstream boundary conditions.

224   HEC-RAS simulated water level was compared with predicted astronomical tide at

225   Washington D.C. Waterfront (NOAA's CO-OPS Station ID 8594900). Initial Manning's n

226   values were assigned based on the calibration provided in the FEMA HEC-RAS model for the

227   upper portion of the model. For the lower portion, we started with a constant Manning's n from

228   the literature (0.025) and then made adjustments until we reached values closer to the NOAA's

229   CO-OPS published tidal amplitudes. In addition to full time series statistical analysis, harmonic

230   analysis of tidal constituents was performed using T_TIDE (Pawlowicz et al. 2002) on HEC-

231   RAS simulated water levels at the Washington Waterfront.

232   *2.1.2   Calibration to Historic Floods and High Water Marks with HEC-RAS*
233   HEC-RAS was further calibrated for various historic freshwater events that caused

234   extensive flooding at Wisconsin Avenue at Washington, D.C. Although flooding on the Potomac

235   has occurred every month of the year, most Potomac River floods occur in spring due to heavy

236   rainfall, sudden or rapid snowmelt and usually last for several days (Doheny 1997). Detailed

237   flow hydrographs are not available for the historic flooding events and only peak flows were

238   available in the literature. Inflow hydrographs for the HEC-RAS model were developed starting

239   with an assumed base flow followed by a symmetric three-day linear rise to the observed peak

240   and subsequent three-day linear fall back to the assumed base flow requiring a total of six days

241   of simulation for each historic flood event. Rise and fall of the Potomac floods over six days are

242   a reasonable approximation of the observed flow hydrographs reported by Doheny (1997).

243   We adjusted the Manning's n values in the upper Potomac channel sections and overbank

244   areas to produce a good fit for the peak stages at Wisconsin Avenue. This final set of calibrated

245   roughness coefficients was used for all subsequent HEC-RAS simulations.

246   *2.1.3   January, 2010 Low Flow Event Validation*
247   The first validation run used 10 days of observed flow and stage data from a low-flow

248   period from January 3, 2009 through January 12, 2009 when water level fluctuation was due

249   almost entirely to tidal effects to validate the simulated propagation of tide. No model parameters

250   (such as roughness) were adjusted during this simulation.

251   *2.1.4   Hurricane Isabel Event in 2003*
252   Additional model validation was performed for the Hurricane Isabel event in 2003.

253   During Isabel, a 1.8 m to 2.4 m (6 to 8 ft) storm tide reached the Washington, D.C. area via the

254   Potomac River, causing flooding in Old Town Alexandria and requiring closure of flood gates at

255   the Washington Harbour Center in Georgetown. Two days later, a second flood wave caused by

256   heavy rain upstream in the Potomac River watershed (NOAA 2009) arrived at Washington

257   Harbor Center. We simulated the Isabel event from September 18, 2003 to September 22, 2003

258   to include both the storm tide and subsequent high river discharge through the Potomac River.

259   ### 2.1.5   *Development of Forecast Guidance Curves*

260   Historically, during high river flow, MARFC utilized empirical guidance curves for

261   forecasting at Wisconsin Avenue. The HEC-RAS model was used to generate forecast guidance

262   curves that were similar to the empirical guidance curve but based on simulated dynamic tide

263   and river flow. The new curves show the ability of the dynamic model to reduce uncertainty

264   compared to the empirical forecasting approach and also show the relative importance of tides at

265   two points of interest in the Washington, D.C. area.

266   ## 2.2   Wind Modeling Experiments for Hurricane Isabel

267   Although the HEC-RAS model accounts for the propagation of the surge-created water

268   level from the Potomac mouth at Lewisetta, the further amplification of that surge by the along-

269   axis winds in the channel itself is not considered in HEC-RAS.

270   ### 2.2.1   *SOBEK 1D Model*

271   To examine the effects of direct wind forcing implemented in a 1D model, we used the

272   SOBEK-Rural 1D-FLOW module, we created the SOBEK implementation by importing the

273   HEC-RAS model into the SOBEK software package. No modifications were made to the

274   bathymetry or model parameters such as friction coefficients. To verify the HEC-RAS to

275   SOBEK conversion, we ran a SOBEK simulation without any wind forcing for the 2003

276   Hurricane Isabel with boundary values and the simulation period all identical to the HEC-RAS

277   model.

278   SOBEK includes a wind friction term in the momentum equation with user specified

279   wind friction coefficients and "wind hiding" factors (to be discussed later). Wind data are input

13

280 as direction and speed for each time step and may be specified for the entire model or individual

281 reaches. The angle between each river reach and the wind direction is used to calculate the wind

282 shear stress along the river.

283 **2.2.2 *ADCIRC 2D Model***

284 We also simulated storm surge during Hurricane Isabel using the two-dimensional

285 ADvanced CIRCulation (ADCIRC) hydrodynamic model (Westerink et al. 1992). ADCIRC

286 simulations were performed using the model domain developed by the NOS VDatum project for

287 the Chesapeake Bay, Delaware Bay, and adjacent coastal water areas (Fig. 3) (Yang et al. 2008).

288 This model grid represents the domain with 318,860 nodes and 558,718 triangular elements and

289 resolves various rivers and small tributaries in the Chesapeake and Delaware Bay.

290 We started with the calibrated ADCIRC model parameters from the VDatum project

291 changed bottom friction coefficients to match surge at the Washington D.C. area. We used lateral

292 viscosity as a constant, 25.0 m s^{-2}, throughout the model domain and a quadratic friction scheme

293 with specified spatially-varying coefficients to calculate bottom friction. The five most

294 significant astronomical tidal constituents (M_2, S_2, N_2, K_1 and O_1) derived from the Western

295 North Atlantic Ocean tidal model (WNATM) provided open-ocean boundary tidal forcing as was

296 specified in the VDatum project (Mukai et al. 2002).

297 For Hurricane Isabel simulations, wind and pressure fields were generated using the

298 Holland parametric wind model (Holland 1980, 2008) included within ADCIRC. The Holland

299 model calculated wind stress and barometric pressure for the ADCIRC simulations based on the

300 best track estimate and cyclone parameters obtained from the National Hurricane Center (NHC).

301   Hindcast surge simulations were for the 4.375 days from September 15, 2003 15:30 GMT

302   to September 20, 2003 0:00 GMT with 40 days of tidal spin up. Time series of wind and water

303   levels were saved at 30 minute intervals.

304   *2.2.3   Wind Data Sources*

305   Operational implementation of a wind forcing term in riverine hydraulic models, will

306   require both observed and forecast wind data. Thus, for Hurricane Isabel simulations we

307   examined the use of two separate sources of wind data: 1) observed wind speed and directions at

308   the CO-OPS stations at Lewisetta and 2) forecast wind speed and direction output from the

309   ADCIRC model. Because the available CO-OPS observed data were limited to point

310   observations, we applied a single direction and speed time series to the entire SOBEK model

311   rather than separate time series to sub-reaches. For consistency between the observed and

312   forecast-based simulations, only the wind time series at a node located near Lewisetta, VA, was

313   extracted from ADCIRC output. Table 3 summarizes the modeling experiments to examine wind

314   effects during Hurricane Isabel. We tested the SOBEK model with no wind, CO-OPS observed

315   wind, CO-OPS observed wind with a "wind hiding" factor of 0.75, and wind produced from

316   ADCIRC runs. The factor of 0.75 was applied to instantaneous (non-averaged) wind

317   observations taken every hour at Lewisetta, VA and was derived purely based on calibration to

318   reproduce the peak surge at Washington Waterfront. Westerink et al. (2008) discuss two physical

319   reasons for needing to reduce observed or simulated wind in hydrodynamic model

320   implementations to predict surge near the coast. One reason relates to the wind temporal

321   averaging scale used to derive surface drag law coefficients. For example, Westerink et al.

322   (2008) report that a 10 minute wind averaging period is suitable for application of Garratt's drag

323   formula (Garratt 1977). Therefore, they adjusted 1 minute winds from a parametric wind model

324   by a factor of 0.893 (from Powell et al. 1996) to apply the drag law correctly. This reduction

325   accounts for the fact that 10-minute temporal averaging produces smaller peak wind values

326   relative to 1-minute averaging. A second physical reason to modify observed wind for use in a

327   model is that wind observed near open water or wind simulated for the open ocean is often

328   reduced by land roughness elements such as trees, topography, buildings, etc. so that the overall

329   effect on water movement is lessened at points farther inland.

330   Although it is unclear from the literature precisely how the instantaneous hourly

331   observations at Lewisetta should be adjusted to apply drag formulas used in SOBEK1D, it seems

332   clear that some adjustment is required. Since Lewisetta, VA, is situated close to the wide

333   Potomac mouth and open water of the Chesapeake Bay, it is likely that our calibrated reduction

334   factor accounts for the effects of land roughness elements found in the more upstream reaches of

335   the model domain.

336   **3   RESULTS AND DISCUSSION**

337   **3.1   Calibration Results**

338   *3.1.1   Tide Propagation*

339   Fig. 4 presents comparisons of the CO-OPS predicted and HEC-RAS simulated water

340   level at Potomac River at Washington D.C. Waterfront (NOAA's CO-OPS Station ID 8594900)

341   for the pure astronomical tide simulation. Comparison of the model simulated water level to CO-

342   OPS predicted tide indicate that tidal amplitude, phase and spring and neap tide modulations

343   were captured by the HEC-RAS model fairly accurately except that HEC-RAS peak simulations

344   precede observed tide peaks by about two hours. We shifted the HEC-RAS time series before

345   statistical analysis to determine series mean differences, root mean square error (RMSE), mean

346   error (ME) and standard deviation (SD) of error at Potomac River at Washington Waterfront.

347   The series mean difference (CO-OPS minus HEC-RAS) was 0.01 m (0.05 ft) and the RMSE was

348   0.05 m (0.16 ft). Table 4 summarizes all of the computed statistics.

349   The T_TIDE analysis showed that the three largest harmonic constituents of tidal

350   variation at Washington Waterfront were the M2 (Principal lunar semidiurnal), S2 (Principal

351   solar semidiurnal) and N2 (Larger lunar elliptic semidiurnal) constituents. Table 5 gives the

352   amplitude difference and phase shift for these constituents and shows close agreement with the

353   CO-OPS observed tides. The largest contribution to the variation in the observed tide is from the

354   M2 constituent with amplitude of 0.41 m (1.35 ft). This is close to the simulated time series M2

355   amplitude of 0.44 m (1.46 ft), a difference of 0.03 m (0.11 ft). The simulated M2 phase is shifted

356   two hours early from the observed.

357   The amplitude and phase differences between HEC-RAS and CO-OPS are similar to the

358   differences reported by Lanerolle et al. (2009) for CBOFS. Both the HEC-RAS model and the

359   CBOFS model have phase errors of about 2 hours (predicting early high tides). More

360   investigation will be required to determine the cause of the phase error in both of these models.

361   *3.1.2   Historic Floods*

362   In total, eight historic flooding events were simulated including the largest flood ever

363   recorded for the Potomac River at Little Falls, the 1936 flood event which had the peak flow of

364   13,450 cms (475,000 cfs). Table 2 and Fig. 5 summarize performance for historical events.

365   Simulated peak errors range from -0.4 m to 0.4 m (-1.34 ft to 1.34 ft) (Table 2). The mean

366   absolute error for peak predictions was 0.25 m (0.82 ft). The correlation between simulated and

367   observed peaks was 0.88 and the R^2 for the 1:1 fit was 0.90.

368   **3.2   HEC-RAS Validation Results**

369   *3.2.1   January, 2010 Low Flow Event*

370   Fig. 6 shows a historical simulation for the January validation event at the Washington

371   Waterfront station. From January 3 to January 12, 2009, water level fluctuated from 0.6 m (2

372   feet) above MSL to 0.8 m (2.5 ft) below MSL and flow varied from 170 cms to 764 cms (6,000

373   cfs to 27,000 cfs). Similar to the tide calibration plot (Fig. 4), HEC-RAS simulates amplitude and

374   water level peaks and troughs reasonably well, but peaks occur about 2 hours early. The

375   difference in series means (observed minus HEC-RAS) was 0.06 m (0.18 ft) and simulation

376   RMSE was 0.12 m (0.38 ft). Table 4 lists the remaining statistics.

377   *3.2.2   Hurricane Isabel Event in 2003*

378   Fig. 7 shows the observed and HEC-RAS simulated water level at the Washington

379   Waterfront station for Hurricane Isabel in 2003. Even though the simulated water level tracked

380   observed water level reasonably well, simulated peak storm tide due to Hurricane Isabel was

381   0.66 m (2.13 ft) lower than the observed data. This is well below the accuracy of surge prediction

382   reported by Cho (2009) and Cho et al. (2011) using the 2D CIPS-ELCIRC model. Cho et al.

383   (2011) reported peak prediction errors of 0.03 m (0.1 ft). With CBOFS we have not been able to

384   make the same comparison at the Washington Waterfront location because CBOFS model

385   boundary does not reach this location; however, downstream comparisons suggest that CBOFS

386   will also predict a more accurate surge similar to CIPS performances.

387   **3.3   Results from Forecast Guidance Curves**

388   The dashed line in Fig. 8 is a quadratic best fit curve for the historic peaks (shown with

389   plus marks) and is similar to the guidance curve that MARFC and the Sterling Weather Forecast

390   Office (WFO) used to manually estimate stage at Wisconsin Avenue as a function of flow at

391   Little Falls prior to the availability of the HEC-RAS model. In this study, we generated the HEC-

392   RAS based traces (gray lines) in Fig. 8 using a series of simulations with a set of constant pre-

393   flood water levels in the tidal zone with the possible intra-tidal range of -0.92 m to 0.92 m (-3 ft

394   to +3 ft) MSL. For each trace, the model is initialized with a low flow value at the upstream end

395   and a fixed elevation between -0.92 m to 0.92 m (-3 and +3 ft) at the downstream end. To

396   generate points along each trace of Fig. 8, the model is run first with a low flow until equilibrium

397   is reached and then a storm event with a peak flow is introduced at the upstream end and the

398   maximum predicted stage at the location of interest (e.g. Wisconsin Avenue) is recorded.

399   Based on these traces, we see that water levels at Wisconsin Avenue may vary

400   substantially depending on pre-flood water level. The smaller range at higher flows indicates

401   (intuitively) that freshwater flow dominates the river stage for high flows. At low flows, the

402   HEC-RAS traces reasonably bound the range of uncertainty in the observed peak flows.

403   Differences in initial tidal level may explain the scatter (uncertainty) in the observations. Using a

404   HEC-RAS model with actual tidal data could reduce the uncertainty in water level forecast

405   relative to the empirical curve method. At very high flows, where there is less scatter in the

406   historic data, the benefits of running the HEC-RAS model to predict stage at Wisconsin Avenue

407   are reduced; however, the HEC-RAS model offers additional benefits such as the ability to

408   produce peak time and stage forecasts at many locations along the lower Potomac, and the ability

409   to produce water surface profiles that can be used to generate flood forecast maps.

410   Fig. 9 compares the effect of initial water level on freshwater events at two locations:

411   Wisconsin Avenue and the Washington Waterfront, 4.8 km (3 miles) down stream. The flatter

412   slope and wider spread of the Washington Waterfront curves in Fig. 9 indicates a substantially

413 greater tidal influence on water levels compared to the Wisconsin gage despite their relatively

414 close proximity.

415 **3.4   Results from Wind Modeling Experiments for Hurricane Isabel**

416   Fig. 10 presents hurricane surge at the Washington Waterfront simulated by the HEC-

417 RAS and SOBEK models without using wind forcing in both models. Without wind forcing,

418 SOBEK produces an almost identical water level peak for Hurricane Isabel. Although the models

419 use the same geometry and roughness parameters, there are discrepancies between HEC-RAS

420 and SOBEK results for moderate to low flows. These are likely due to differences in methods to

421 compute conveyance and numerical solution algorithms used by SOBEK and HEC-RAS. Peak

422 surge estimated by HEC-RAS and SOBEK without wind were 2.0m (6.59 ft) and 2.06 m (6.75

423 ft), respectively. Time of peak surge estimated by HEC-RAS was 05 GMT while SOBEK was

424 05:30 GMT. Differences between the two peak surge heights was -0.05 m (-0.16 ft) and the time

425 difference was about 30 min. The rising and falling shape of the surge hydrographs appear

426 similar.

427   Fig. 11 presents ADCIRC simulated peak surge at Washington Waterfront. Computed

428 peak surge was 2.6 m (8.45 ft) on 19 September 2003 at about 05 GMT compared to the 2.65 m

429 (8.7 ft) observed peak. Time of the peak was similar to the HEC-RAS model and was about 4

430 hours early. Since ADCIRC simulated surge peak was close to the observed, we used ADCIRC

431 generated wind forcing (wind speed and direction) along with ADCIRC simulated water level as

432 another scenario to force the SOBEK model (Table 3).

433   Fig. 12 shows a snapshot of the ADCIRC generated directional wind pattern when wind

434 direction was favorable for propagating water into the Chesapeake Bay and into the Potomac

435 River. Fig 13 shows the magnitude of the wind speed simulated by ADCIRC along the Potomac

436   River along with CO-OPS wind at Lewisetta. ADCIRC peak wind speeds at Lewisetta and

437   Colonial Beach are similar, about 22 m/s (49.2 mile/hr). We used ADCIRC wind at Lewisetta,

438   VA, for SOBEK applications. Wind values at Wisconsin Avenue are notably less than at the

439   other stations with open ocean exposure, justifying our empirically reduced Lewisetta wind. Fig.

440   14 illustrates that the strongest winds blew during the 12 hours leading up to the peak surge.

441   These winds were roughly aligned with the axis of the Potomac River (coming from 90 degrees

442   to 180 degrees relative to North), allowing optimal conditions for surge propagation from the

443   Chesapeake Bay and toward Washington D.C.

444   Fig. 15 shows results from the SOBEK model with three separate wind forcings. Table 3

445   includes peak level and timing statistics for the simulations. Simulated peak level errors for CO-

446   OPS wind, 0.75*CO-OPS wind, and ADCIRC wind cases are +0.70 m (2.3 ft), -0.08 m and -0.18

447   m respectively. For all three simulations time to peak did not change more then 30 min.

448   Therefore, while application of wind changed peak surge, no significant improvements were

449   observed in estimating time to peak surge. Interestingly, peak surge predicted by the SOBEK

450   implementation with no wind was closer to observed than peak surge predicted when applying

451   raw CO-OPS wind from Lewisetta to the entire model. The SOBEK no-wind case

452   underestimated the peak by -0.57 m (1.9 ft) and the SOBEK CO-OPS wind case overestimated

453   by +0.7 m (2.3 ft). While these results give us confidence that the magnitude of a wind forcing

454   term in a 1D hydraulic model is an important factor in modeling surge, it also highlights the

455   challenges in properly implementing and parameterizing the wind term. Further work can be

456   done to improve the physical inputs and reduce reliance on calibration. For example, a modeler

457   could use gridded wind data for both forecast and observed time periods when available, or

458   estimating wind reduction factors using techniques similar to those described by Westerink et al.

459   (2008).

460   The peak error from SOBEK with ADCIRC wind case was 0.18 m (0.6 ft) compared with

461   0.01 m (0.03 ft) for the ADCIRC simulation (Figure 11). We suspect the differences are mostly

462   due to differences in the parameterization of the drag coefficients between ADCIRC and SOBEK

463   and the fact that ADCIRC uses a spatially varying wind field, and not differences between 1D

464   and 2D hydrodynamic calculations. Future work is needed to confirm this hypothesis. These

465   results highlight the need to develop consistent wind pre-processing and parameterization

466   procedures for both observed and forecast wind fields for operational implementation of 1D

467   models.

468   For all the modeling scenarios, Table 3 reports the peak flows into the Potomac River

469   from the Chesapeake Bay during Hurricane Isabel. While we do not have observed data to

470   validate these flows, the flow results among models are consistent with the respective physical

471   inputs and stage forecasts. As expected, the SOBEK simulation with observed CO-OPS wind has

472   a much higher inflow than SOBEK simulation which uses a reduction factor of 0.75. The

473   reductions in flow are comparable among different models when moving upstream. For example,

474   inflows with observed CO-OPS wind are consistently higher than those from simulation which

475   uses a shielding factor of 0.75 when moving from the mouth of the river at Lewisetta to near the

476   midpoint at Newburg to almost the upstream end at Alexandria. On average only 3% of the peak

477   inflow to the Potomac from storm tide reaches Alexandria, VA. Despite this dramatic inflow

478   reduction, storm tide still plays a dominant role in water levels in the Washington, D.C region for

479   this event.

22

4   CONCLUSIONS AND RECOMMENDATIONS

This 1D HEC-RAS model of the tidal Potomac River is capable of simulating water levels from the Potomac mouth at the Chesapeake Bay upstream past Washington, D.C. to near the Little Falls pump station. The simulation results suggests that implementing new 1D models with boundary conditions derived from 2D/3D models can be a technically sound and viable approach for reducing the operational flood forecast service gaps that exist for coastal rivers throughout the Nation. The NWS MARFC has begun testing this model for operational forecasting within CHPS. The HEC-RAS model offers an enhanced capability over an existing empirical technique for predicting flood stages at Wisconsin Avenue in Washington, D.C.

The HEC-RAS boundary condition requirements are relatively simple for the lower Potomac implementation: observed and forecast discharge time series at upstream boundaries and observed and forecast stage time series at the downstream boundary. At the downstream boundary, observed water level can be obtained from the Lewisetta CO-OPS station and forecast water level from one of several operational estuary-ocean models: CBOFS, ET Surge, or ESTOFS. Forecasters can configure CHPS to compare results using the different available boundary conditions in real-time. This loose coupling of operational HEC-RAS models and one or more operational estuary-ocean models provides a baseline, operational river-estuary-ocean forecasting capability which is relatively easy to implement and provides a good reference against which more advanced modeling techniques (e.g. detailed 2D/3D estuary ocean models extended farther upstream) can be measured in the future.

We calibrated and validated the HEC-RAS model over a wide range of conditions including a time period dominated by tide, a period with both tidal and freshwater flow influence, historic freshwater floods, and an extreme storm surge event. For pure tidal

503 simulation, RMSE for simulations at Washington Waterfront was 0.05 m. For the period with

504 mixed tidal and freshwater flows, RMSE was 0.12 m. For eight historic flood events, peak

505 prediction errors at Wisconsin Avenue were all less than 0.41 m and the mean absolute error was

506 0.25 m. Simulation error for the Hurricane Isabel peak surge at the Washington Waterfront was

507 0.65 m. Like the water level prediction, the peak time prediction error for the surge event (4

508 hours) was also larger than prediction errors for moderate flow and tidal events (2 hours).

509   The HEC-RAS simulations showed promising performance for freshwater and tide

510 dominated events, but less accurate performance for the heavily wind-forced hydraulics during

511 Hurricane Isabel. The lower performance in predicting peak surge during Hurricane Isabel is not

512 surprising given that HEC-RAS does not include an explicit wind forcing term. We simulated

513 "HEC-RAS plus wind" model by running SOBEK 1D model with identical geometry but

514 incorporating wind forcing in the model. We ran a SOBEK model with several wind scenarios to

515 confirm whether wind can account for this level of error in a 1D model. Basic runs in SOBEK

516 using the same model geometry as HEC-RAS confirmed that the two models produced similar

517 peaks without wind. SOBEK runs with wind showed that the observed peak surge at Washington

518 Waterfront could be easily matched, but only after the wind reduction factor was calibrated.

519 However, the SOBEK models with wind did not substantially reduce peak timing error for

520 Hurricane Isabel. For these runs, SOBEK wind inputs were based on a single time-series of

521 observed wind from the CO-OPS gauge at Lewisetta.

522   To gain additional understanding, we ran a 2D ADCIRC model in simulation mode for

523 Hurricane Isabel. This model accurately predicted the peak surge level at Washington Waterfront

524 after spatially variable bottom friction factors were calibrated. Similar to SOBEK and HEC-

525 RAS, the ADCIRC model also showed about a four hour peak timing error. The ADCIRC

526 implementation uses a two-dimensional, parametric wind field rather than point observed data.

527 Operational implementation of a 1D hydraulic model with a wind forcing term requires

528 both observed and forecast wind data. Our tests running SOBEK using "forecast" wind from

529 ADCIRC output suggest that a pragmatic option to obtain forecast winds in operations is to

530 leverage pre-processed wind fields from operational estuary-ocean models such as ADCIRC

531 (used as the basis for ESTOFS). However, modelers must ensure that the same wind reduction

532 factors and drag coefficient parameterizations are applied to both observed and forecast winds.

533 To facilitate this, appropriate wind pre-processing tools need to be developed for operational

534 implementation.

535 Given that NWS RFCs are already heavily invested in learning and implementing HEC-

536 RAS models, our results suggest that adding a wind modeling capability into HEC-RAS (similar

537 to that in SOBEK) could provide immediate benefits by enhancing NWS RFC forecasting

538 capabilities along stretches of fourteen coastal rivers where HEC-RAS implementations are in

539 progress or planned. The marginal benefit for each implementation will depend on a variety of

540 factors. A key factor will be the length of river modeled. For shorter reaches, the wind effects

541 embedded in the boundary water level data may be sufficient for surge prediction upstream.

542 However, forecasts for longer reaches (like the lower Potomac) may be substantially improved

543 due to wind effects along the reach.

544 Even given such a new wind modeling capability, more research is needed to guide

545 operational implementation. For our Potomac River implementation, there is a high degree of

546 uncertainty in our calibrated wind reduction factor based on only one event. Given the low

547 computational requirements of 1D models, it should be relatively straightforward to calibrate

548 wind parameters using multiple-year time series of wind data. This approach, however, must be

549 combined with other techniques for extreme events for which calibration data are limited. To

550 improve on the approach we have taken, we recommend using spatially variable wind fields that

551 more accurately describe wind variation over the model domain when possible or deriving wind

552 reduction factors based on physical data, e.g. using techniques described by Westerink et al.

553 (2008).

554

562

563 **6   REFERENCES**

564   Cho, K.-H. (2009). "A numerical modeling study on barotropic and baroclinic responses of the
565   Chesapeake Bay to hurricane events." Ph.D. Dissertation, College of William and Mary,
566   Williamsburg, Virgina.
567   Cho, K.-H., Wang, H. V., Shen, J., Valle-Levinson, A., and Boicourt, W. C. (2011). "Modeling
568   Study on Baroclinic Response of the Chesapeake Bay to Hurricane Events Floyd and
569   Isabel." Submitted Manuscript, Maryland.
570   Deltares. (2011). "SOBEK Suite."
571   <http://www.deltaressystems.com/hydro/product/108282/sobek-suite> (Nov. 7, 2011).
572   Doheny, E. (1997). *Flood-hydrology data for the Potomac River and selected tributaries in the*
573   *vicinity of the Chesapeake and Ohio Canal National Historical Park, Maryland, West*
574   *Virginia, and the District of Columbia*. USGS Open-File Report, U.S. Geological Survey,
575   Baltimore, Maryland.
576   Federal Emergency Management Agency (FEMA). (2010). *Flood Insurance Study: District of*
577   *Columbia, Washington, D.C.* Flood Insurance Study 110001V000A, Federal Emergency
578   Management Agency, Washington, D.C., 93.
579   Fread, D. L., and Lewis, J. M. (1985). "Real-Time Hydrodynamic Modeling of Coastal Rivers."
580   *Applications of Real-Time Oceanographic Circulation Modeling: Symposium*
581   *Proceedings*, B. B. Parker, ed., Marine Technology Society, Washington, D.C., 269-284.
582   Garratt, J. R. (1977). "Review of Drag Coefficients over Oceans and Continents." *Monthly*
583   *Weather Review*, 105(7), 915-929.
584   Holland, G. J. (1980). "An Analytic Model of the Wind and Pressure Profiles in Hurricanes."
585   *Monthly Weather Review*, 108(8), 1212-1218.
586   Holland, G. J. (2008). "A Revised Hurricane Pressure–Wind Model." *Monthly Weather Review*,
587   136(9), 3432-3445.
588   Jelesnianski, C. P., Chen, J., and Shaffer, W. A. (1992). *SLOSH: sea, lake, and overland surges*
589   *from hurricanes*. NOAA technical report NWS 48, National Oceanic and Atmospheric
590   Administration, Silver Spring, Maryland, 65.
591   Kim, S.-C., Chen, J., and Shaffer, W. A. (1996). "An operational Forecast Model for
592   Extratropical Storm Surges along the U.S. East Coast." *Conference on Coastal Oceanic*
593   *and Atmospheric Prediction*, American Meteorological Society, Boston Mass., 281-286.
594   Lanerolle, L. W. J., Patchen, R. C., and Aikman, F. (2009). "The Second Generation Chesapeake
595   Bay Operational Forecast System (CBOFS2): A ROMS-Based Modeling System."
596   *Estuarine and Coastal Modeling*, ASCE, Seattle, Washington, 37.
597   Maryland Department of the Environment (MDE), and District of Columbia Department of the
598   Environment - Natural Resources Administration (D.C. DE-NRA). (2007). *Total*
599   *Maximum Daily Loads of Sediment/Total Suspended Solids for the Anacostia River*
600   *Basin, Montgomery and Prince George's Counties, Maryland and the District of*
601   *Columbia.* Total Maximum Daily Load (TMDL) Study, Maryland Department of the
602   Environment, Baltimore, Maryland, 78.
603   Moreda, F., Gutierrez, A., Reed, S., and Aschwanden, C. (2009). "Transitioning NWS
604   Operational Hydraulics Models from FLDWAV to HEC-RAS." *World Environmental*
605   *and Water Resources Congress 2009: Great Rivers*, S. Steve, ed., ASCE, Reston,
606   Virginia, 292.

607 Mukai, A. Y., Westerink, J. J., Luettich Jr., R. A., and Mark, D. (2002). *Eastcoast 2001, A Tidal*
608   *Constituent Database for Western North Atlantic, Gulf of Mexico, and Caribbean Sea*.
609   Coastal Inlets Research Program ERDC/CHL TR-02-04, U.S. Army Corps of Engineers,
610   Washington, D.C., 196.
611 NOAA. (2009). "A vision for NOAA's Coast, Estuary, River Information Services (CERIS)."
612   NOAA Internal Draft 1.
613 NOAA Coast Survey Development Lab. (2011). "Ocean Prediction Center - ESTOFS Storm
614   Surge Guidance Areas." *Ocean Prediction Center*,
615   <http://www.opc.ncep.noaa.gov/estofs/estofs_surge_info.shtml> (Oct. 26, 2011).
616 Pawlowicz, R., Beardsley, B., and Lentz, S. (2002). "Classical tidal harmonic analysis including
617   error estimates in MATLAB using T_TIDE." *Computers & Geosciences*, 28(8), 929-937.
618 Powell, M. D., Houston, S. H., and Reinhold, T. A. (1996). "Hurricane Andrew's Landfall in
619   South Florida. Part I: Standardizing Measurements for Documentation of Surface Wind
620   Fields." *Weather and Forecasting*, 11(3), 304-328.
621 Roe, J., Dietz, C., Restrepo, P., Halquist, J., Hartman, R., Horwood, R., Olsen, B., Opitz, H.,
622   Shedd, R., and Welles, E. (2010). "NOAA's Community Hydrologic Prediction System."
623   *Proceedings of the 2nd Joint Federal Interagency Conference (9th Federal Interagency*
624   *Sedimentation Conference and 4th Federal Interagency Hydrologic Modeling*
625   *Conference)*, Advisory Committee on Water Information (ACWI), Las Vegas, NV.
626 Schureman, P. (1941). *Manual of Harmonic Analysis and Prediction of Tides*. Special
627   Publication, U.S. Government Printing Office, Washington, D.C.
628 Shchepetkin, A. F., and McWilliams, J. C. (2005). "The regional oceanic modeling system
629   (ROMS): a split-explicit, free-surface, topography-following-coordinate oceanic model."
630   *Ocean Modelling*, 9(4), 347-404.
631 Westerink, J. J., Luettich Jr., R. A., Baptista, A. M., Scheffner, N. W., and Farrar, P. (1992).
632   "Tide and Storm Surge Predictions Using Finite Element Model." *Journal of Hydraulic*
633   *Engineering*, 118(10), 1373.
634 Westerink, J. J., Luettich Jr., R. A., Feyen, J. C., Atkinson, J. H., Dawson, C., Roberts, H. J.,
635   Powell, M. D., Dunion, J. P., Kubatko, E. J., and Pourtaheri, H. (2008). "A Basin- to
636   Channel-Scale Unstructured Grid Hurricane Storm Surge Model Applied to Southern
637   Louisiana." *Monthly Weather Review*, 136(3), 833-864.
638 Yang, Z., Myers, E. P., Wong, A. M., and White, S. A. (2008). *Vdatum for Chesapeake Bay,*
639   *Delaware Bay, and Adjacent Coastal Water Areas: Tidal Datums and Sea Surface*
640   *Topography*. NOAA Technical Memorandum NOS CS 15, National Oceanographic and
641   Atmospheric Administration, Silver Spring, Maryland, 120.
642 Zhang, A., Hess, K. W., and Aikman, F. (2010). "User-based skill assessment techniques for
643   operational hydrodynamic forecast systems." *Journal of Operational Oceanography*,
644   3(2), 11-24.
645 Zhang, Y., Baptista, A. M., and Myers, E. P. (2004). "A cross-scale model for 3D baroclinic
646   circulation in estuary–plume–shelf systems: I. Formulation and skill assessment."
647   *Continental Shelf Research*, 24(18), 2187-2214.
648
649

650

Table 1. Existing NOAA Operational Models in the Chesapeake Bay Region

Model	Lead Organization	Purpose and additional notes
SLOSH (Sea, Lake and Overland Surges from Hurricanes)	NOAA/NWS/NHC	Storm surge during hurricanes and tropical storms (event-based and generated for discrete basins)
ETSurge (SLOSH-based Extratropical Surge)	NOAA/NWS/MDL http://www.nws.noaa.gov /mdl/etsurge/	Continuous water level prediction available for entire Gulf, East, and West coasts including Alaska
ESTOFS (ADCIRC-based Extratropical Surge and Tide Operational Forecast System)	NOAA/NWS/NCEP	Continuous water level prediction for East and Gulf coasts. Higher resolution in some areas than ETSurge but not currently as extensive inland.
CBOFS (ROMS-based Chesapeake Bay Operational Forecast System)	NOAA/CO-OPS	Tide and current forecasts for navigational community in the Chesapeake Bay.

652

Table 2. List of historic flood events caused by freshwater flooding and hurricanes and the corresponding HEC-RAS prediction errors.

Date	Event type	Peak Flow @ Little Falls [cms]	High Water @ Wisconsin Ave. [m MSL]		
			Observed	HEC-RAS	Prediction Error
March 19, 1936	Freshwater	13,450	4.8	5.2	-0.3
October 17, 1942	Freshwater	11,525	5.0	4.6	0.4
June 24, 1972 (from Hurricane Agnes)	Freshwater	9,458	4.3	3.9	0.4
January 21, 1996	Freshwater	9,231	3.4	3.8	-0.4
April 28, 1937	Freshwater	8,778	3.9	3.7	0.3
November 7, 1985	Freshwater	8,297	3.2	3.4	-0.3
September 8, 1996	Freshwater	7,419	3.3	3.2	0.1
January 27, 1910	Freshwater	4,417	1.9	2.0	-0.1
September 21, 2003	Hurricane Isabel*	4,729	2.7	2.00	-0.66

655   * At the CO-OPS station at Washington Waterfront

Table 3. Description of model simulation scenarios for Hurricane Isabel along with peak surge water level, timing and inflow results.

Model	Upstream Boundary Condition (at Little Falls)	Downstream Boundary Condition (at Lewisetta)	Wind Forcing	Peak surge error [m]	Peak timing error [hours]	Qmax Lewisetta, VA [cms]	Qmax Newburg, MD [cms]	Qmax Alexandria, VA [cms]
HEC-RAS	Obs flow	CO-OPS observed stage	No Wind	-0.66	-3	34,141	17,245	1,133
SOBEK	Obs flow	CO-OPS observed stage	No Wind	-0.57	-4	35,000	19,000	1,200
ADCIRC	No River flow at Upstream locations	Ocean tide from ADCIRC database (at Ocean Boundary)	Holland wind Model	0.01	-4	47,500	28,100	1,000
SOBEK	Obs flow	CO-OPS observed stage	CO-OPS observed wind at Lewisetta	0.72	-4.5	53,000	28,000	1,700
SOBEK	Obs flow	CO-OPS observed stage	75% scaled CO-OPS observed wind at Lewisetta	0.08	-4	44,000	22,001	1,300
SOBEK	Obs flow	WL from ADCIRC	Wind from ADCIRC at Lewisetta (Holland Wind Model)	0.18	-5	49,000	21,000	1,500

Table 4. HEC-RAS statistics comparing simulated and reference time series for the astronomical tide calibration and January 2009 low-flow validation simulations at the Washington Waterfront station.

Simulation	Peak difference [hr]	Series mean difference [m] (reference minus simulated)	RMSE [m]	Mean Error [m]	SD [m]
Astronomical tide calibration	-2	0.01	0.05	0.04	0.03
Jan-09	-2	-0.06	0.12	0.09	0.07

Table 5. Tidal harmonic analysis with amplitude referenced to mean seal level (MSL) for three major tidal constituents at Washington Waterfront. Negative sign in phase indicated peak tide in HEC-RAS model leads CO-OPS tide.

Constituent	Constituent amplitude [meters]			Phase Difference [hours]
	CO-OPS (Obs.)	HEC-RAS simulated	Difference	
M2	0.41	0.44	-0.03	-1.6
N2	0.08	0.06	0.02	-2.0
S2	0.05	0.05	0.00	0.9
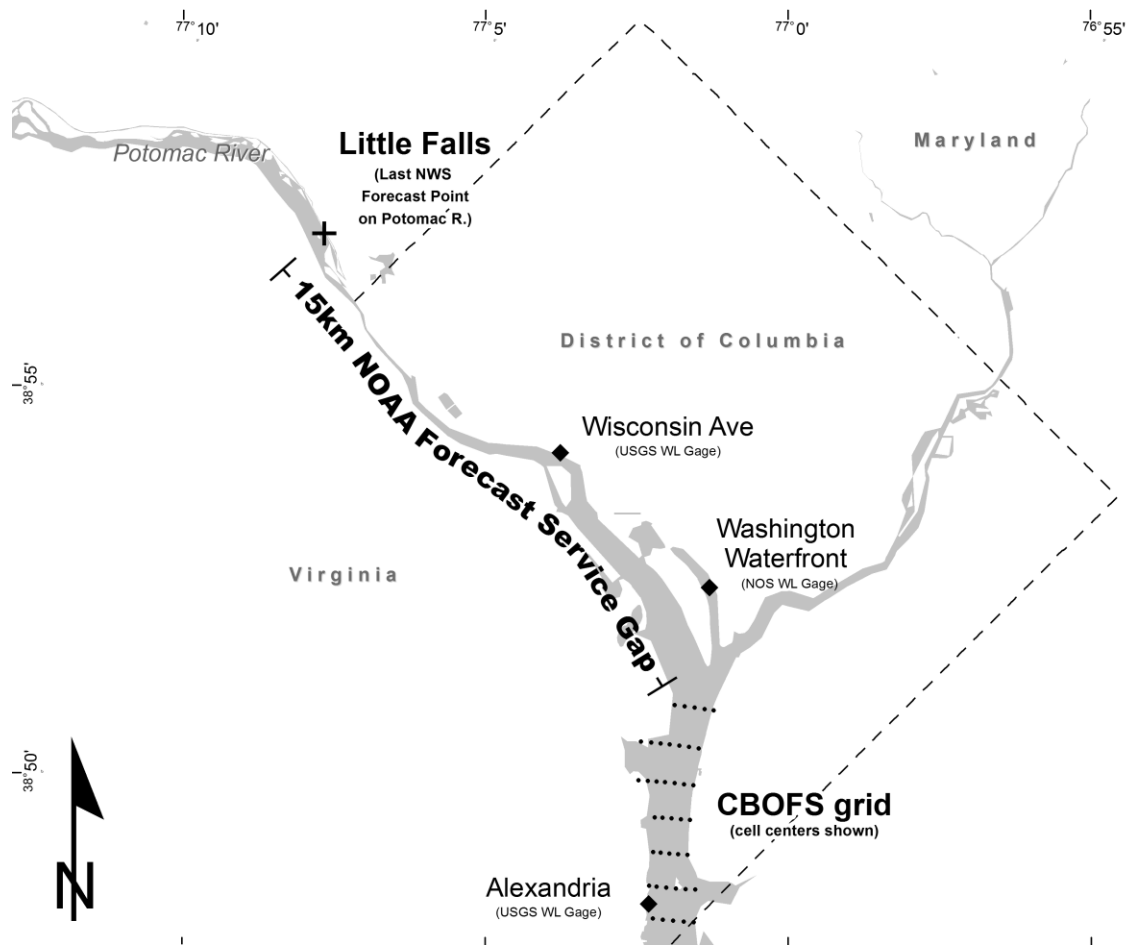
Figure 1. Location of river stage forecast service gap in upper part of the tidal Potomac River near Washington, D.C. The NWS forecast point at Little Falls is approximately 15 kilometers (nine miles) upstream of the existing NOS CBOFS model domain. The CBOFS inflow boundary condition is determined nominally by the Little Falls gage but the geographic location of the upstream point of the domain is not at that location.
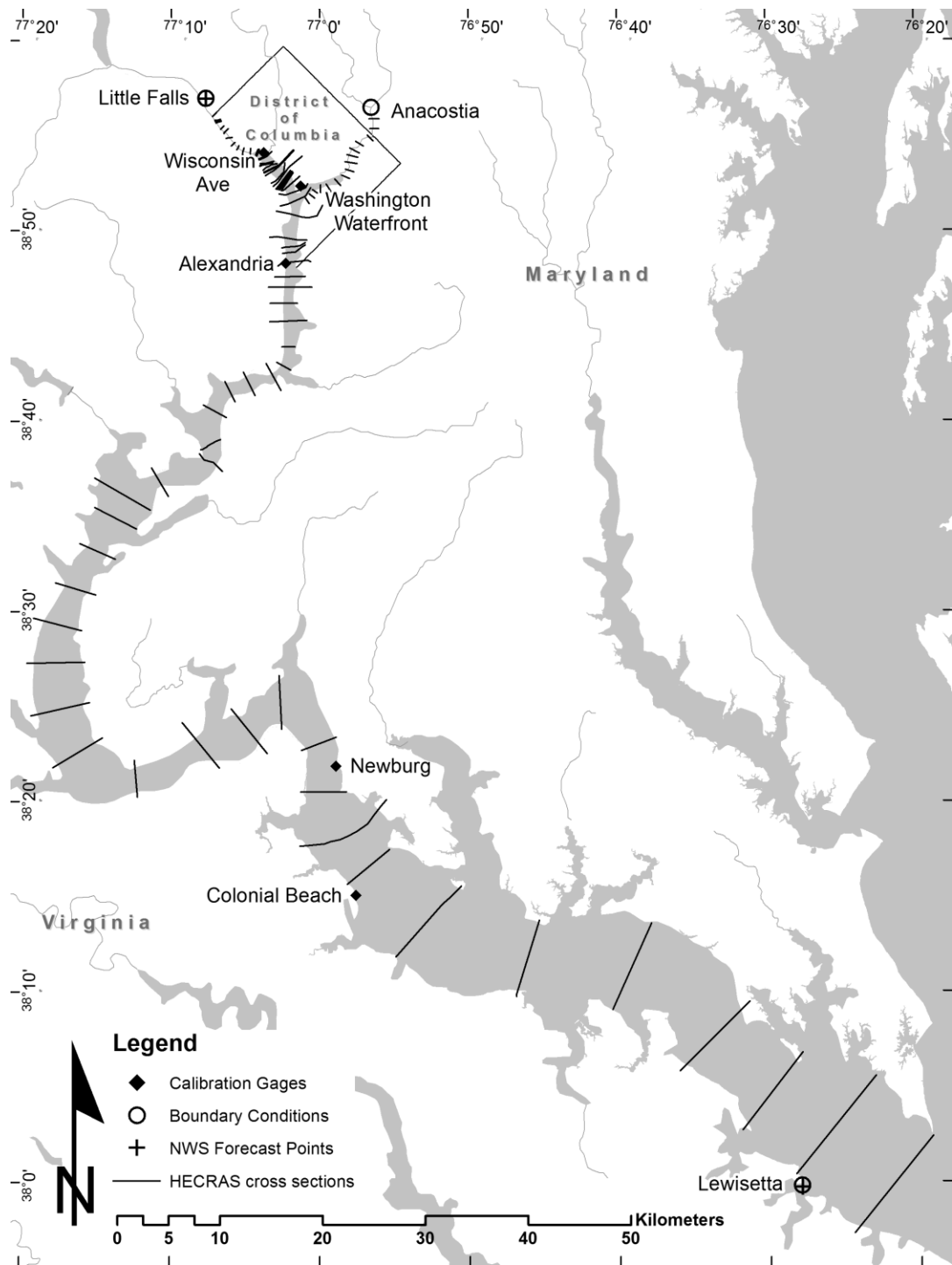
Figure 2. Map of the tidal Potomac River and the Anacostia River within the Chesapeake Bay estuary indicating the extent of the HEC- RAS and SOBEK model domain.
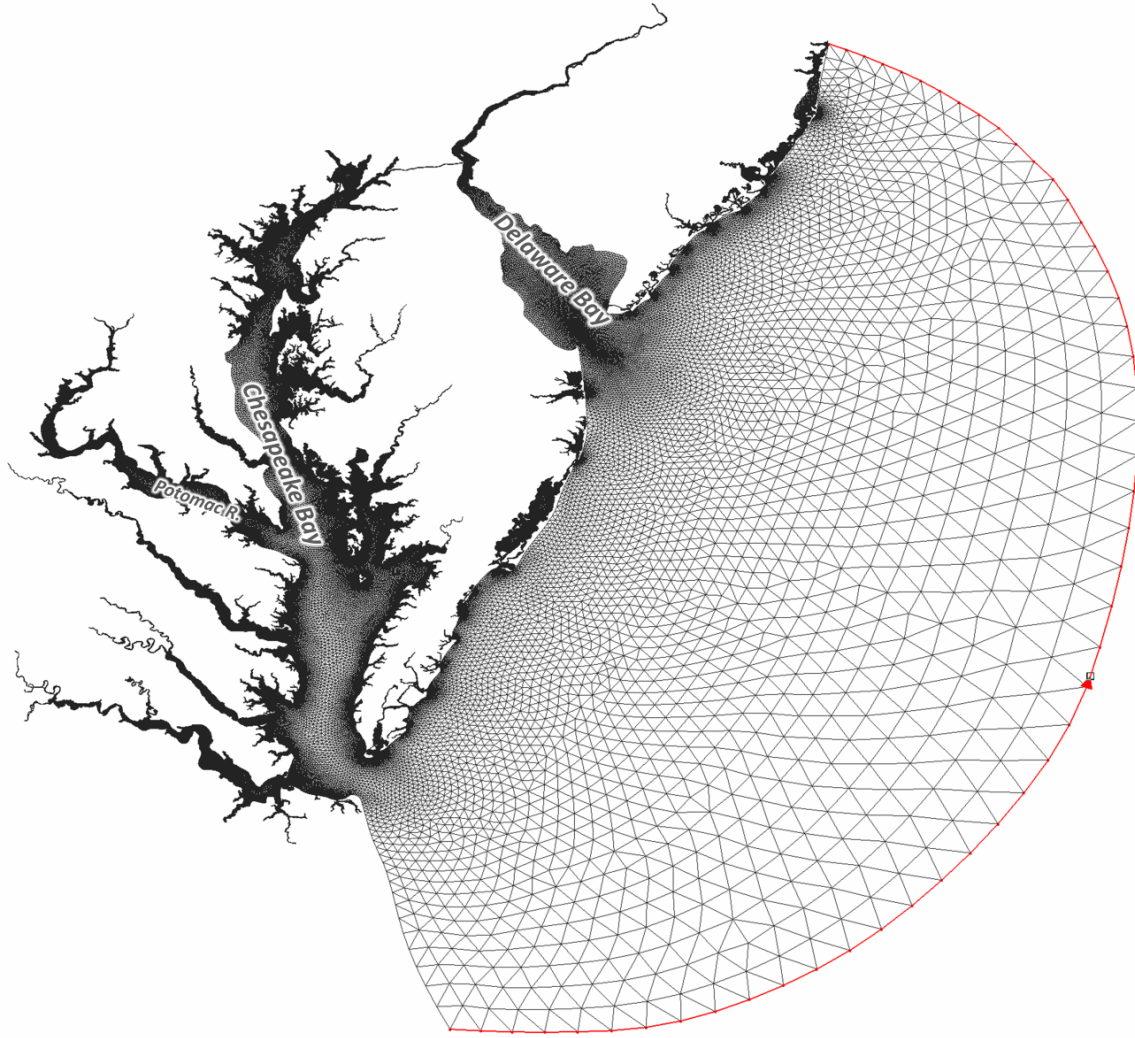
Figure 3. ADCIRC Finite element grid as obtained from the VDatum Study. The open ocean boundary is modeled along the semi-circular curve along the right-hand side of the domain. The grid accurately resolves Chesapeake Bay, Delaware Bay and various coastal rivers.
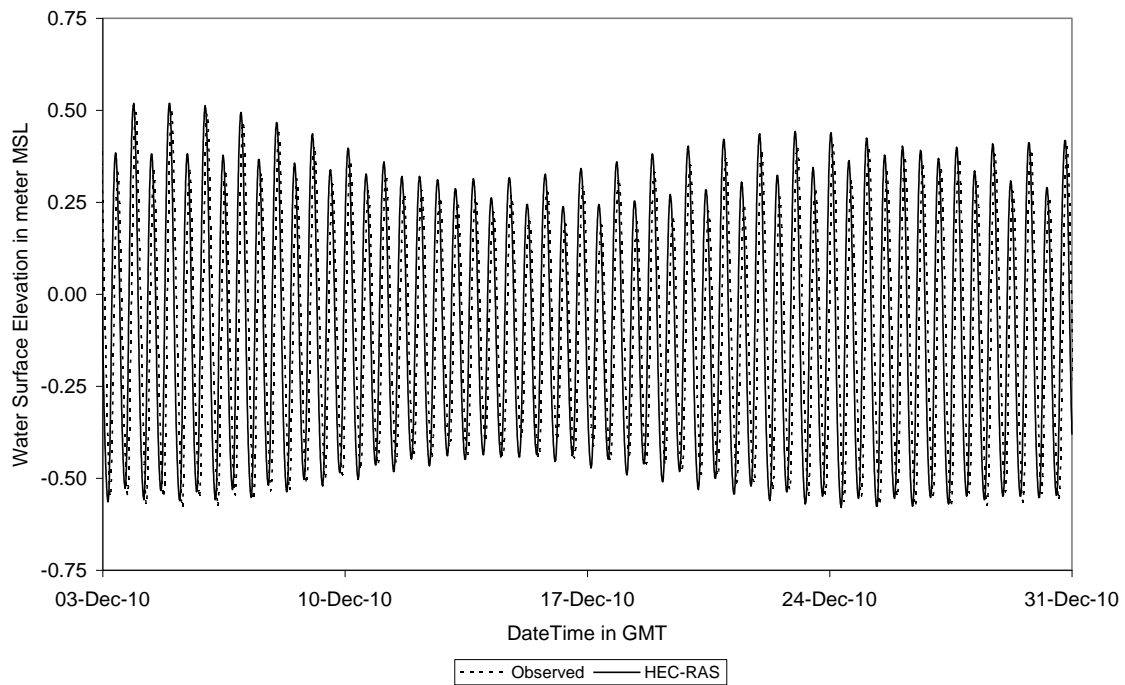
Figure 4 Comparison of HEC-RAS simulated and observed tidal water level at Washington Waterfront for the December 2010 simulation.
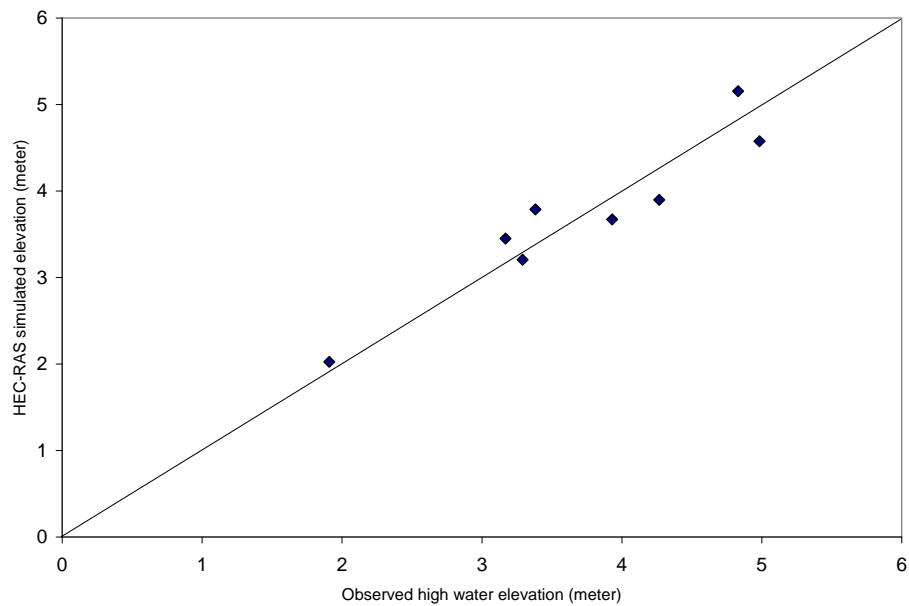
Figure 5 HEC-RAS simulated peaks compared to observed for historic flood events.
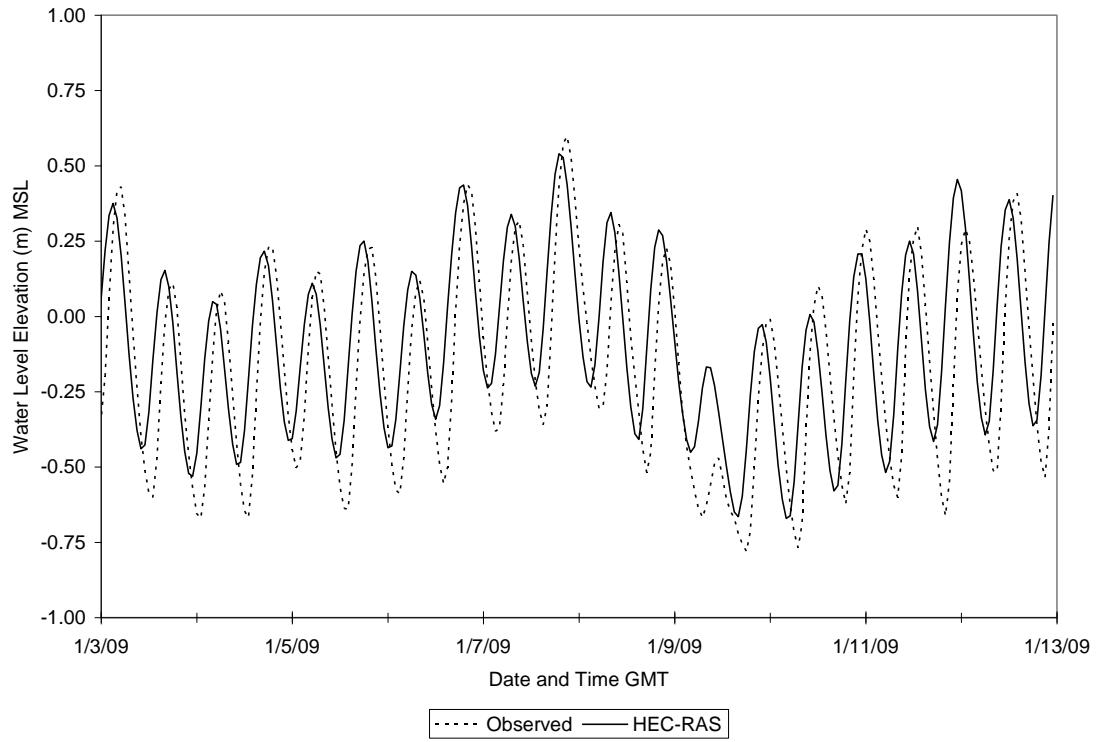
Figure 6. Comparison of the HEC-RAS simulated and observed water levels at the Washington Waterfront for January 3, 2009 to January 13, 2009.
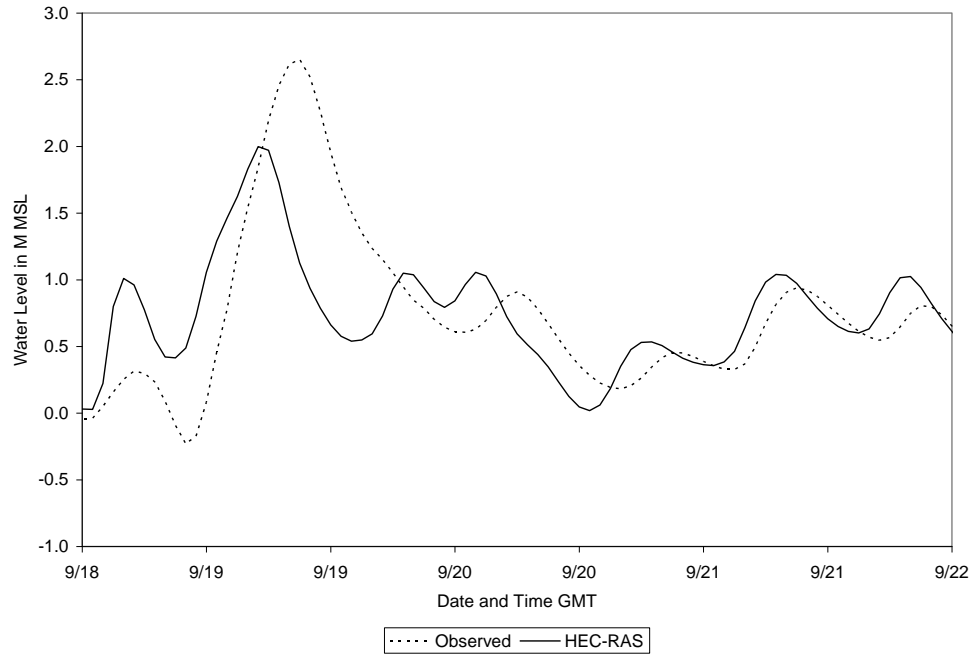
Figure 7. Comparison of the HEC-RAS simulated water level to observed water level at Washington Waterfront for the 2003 Hurricane Isabel.
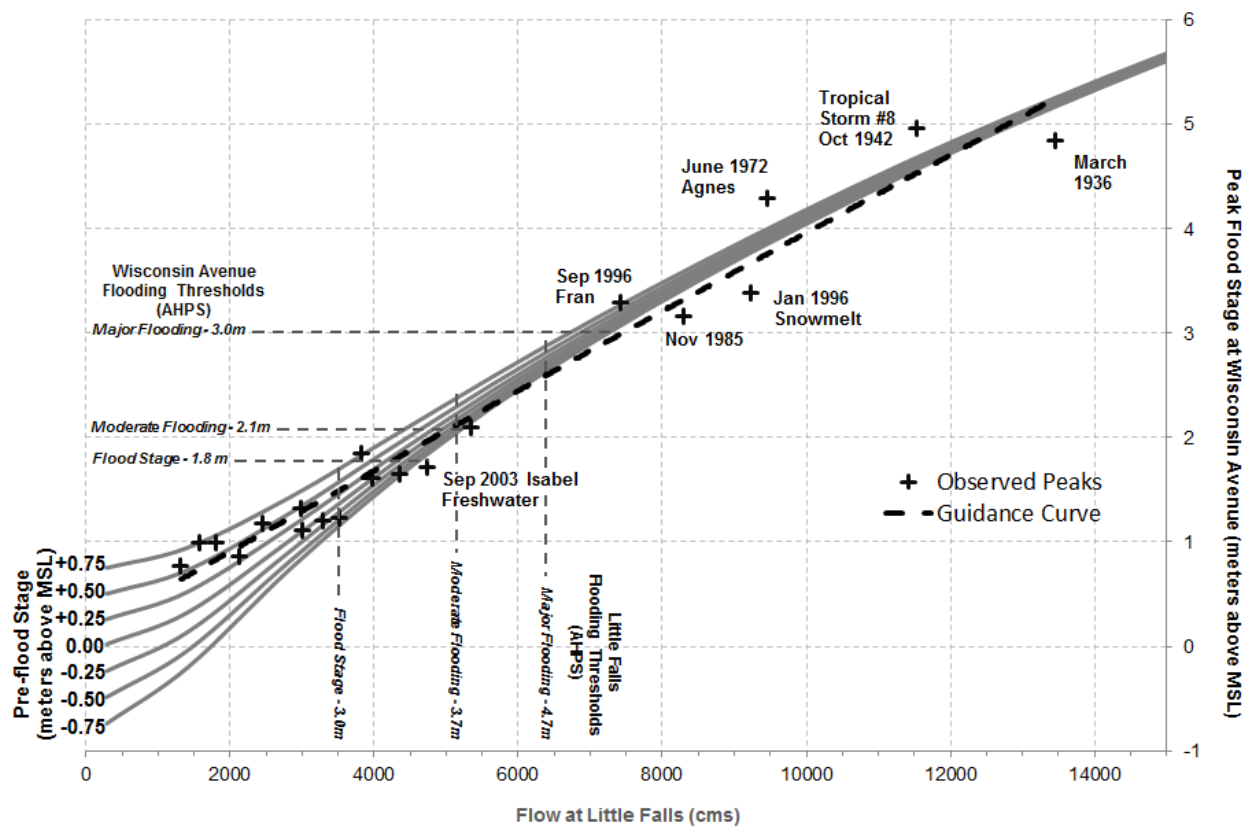
Figure 8. HEC-RAS simulations overlaid on guidance lookup curve developed at the MARFC for forecasting stages at Wisconsin Avenue (dashed line) and historical events (plus signs).
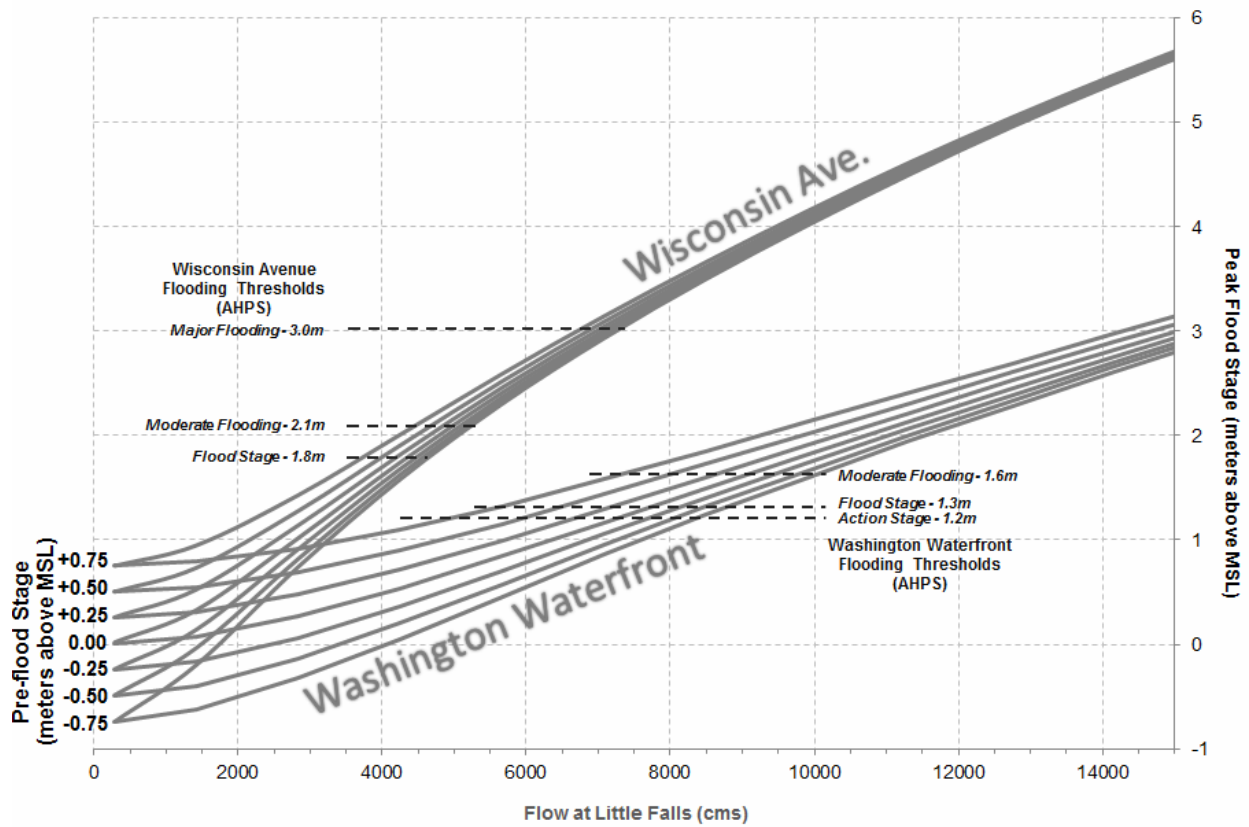
Figure 9. Comparison of influence of initial tidal stage on final flood elevation at Washington Waterfront and Wisconsin Avenue for freshwater events.
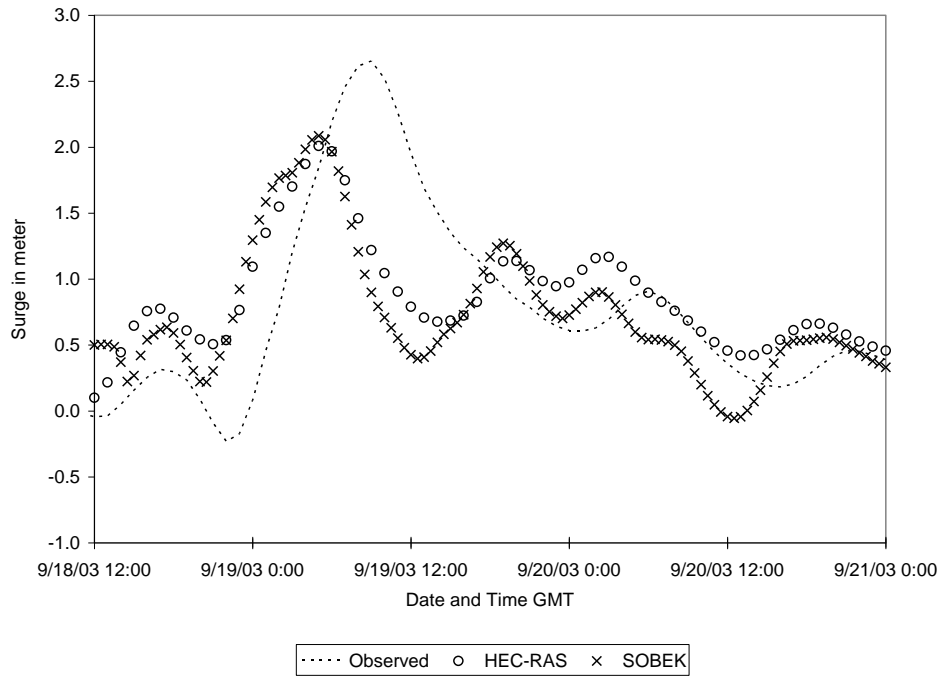
Figure 10. Hurricane Isabel surge at the Washington Waterfront simulated by HEC-RAS and SOBEK model without wind forcing.
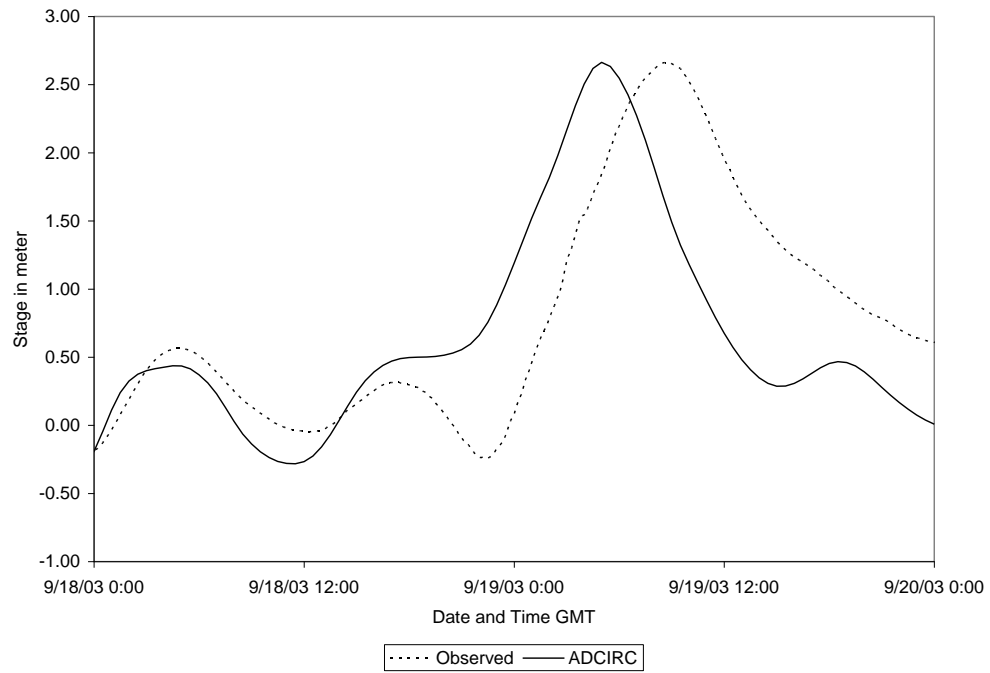
Figure 11. ADCIRC simulated surge during for Hurricane Isabel at Washington Waterfront.
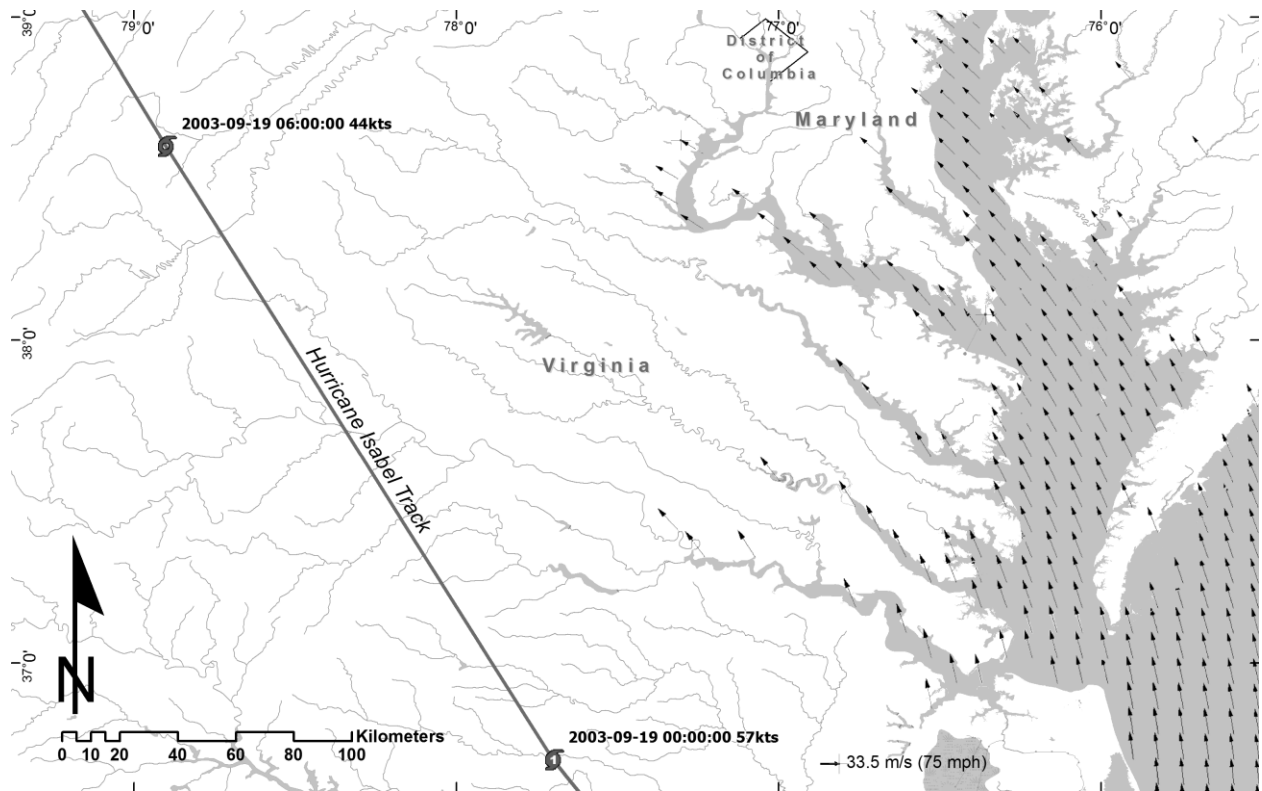
Figure 12. Hurricane Isabel wind used by ADCIRC model at 00:00 GMT, 19 September 2003. Best-track position of hurricane Isabel passing through central VA is indicated with GMT time and maximum wind speed in knots. Note curvature of wind field around hurricane center. Also note that the wind field is generally aligned along the long axes of both Chesapeake Bay and the lower Potomac River channel.
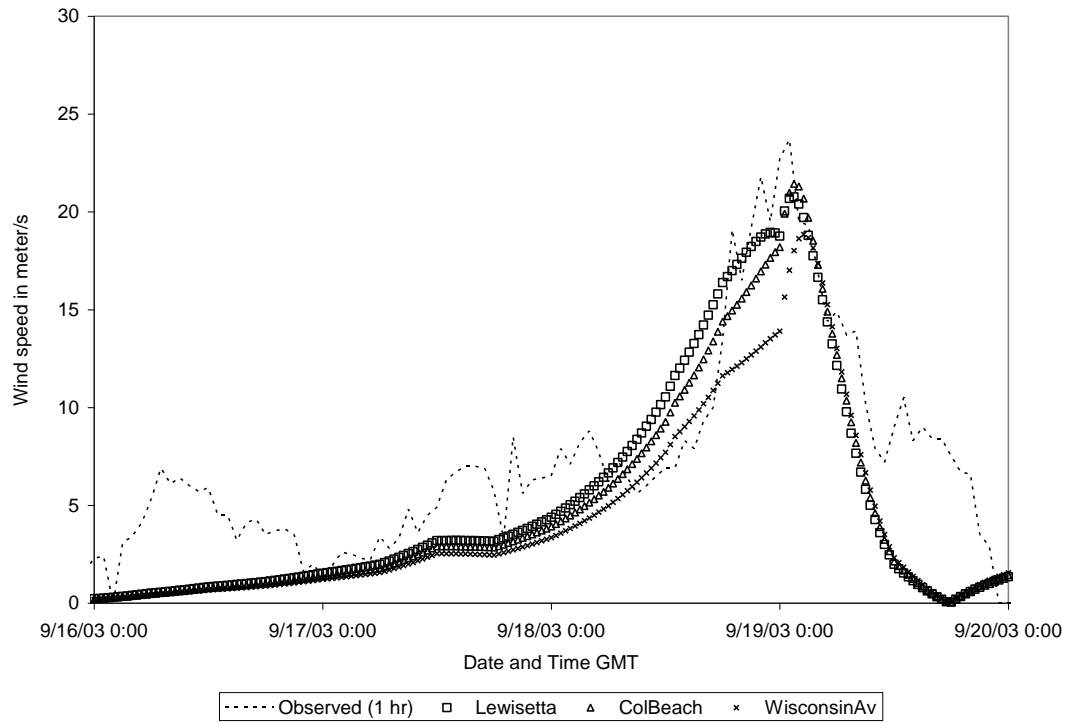
Figure 13. Wind speed as derived from the output from the ADCIRC model at several locations along the tidal Potomac River. CO-OPS observed wind at Lewisetta is also shown.
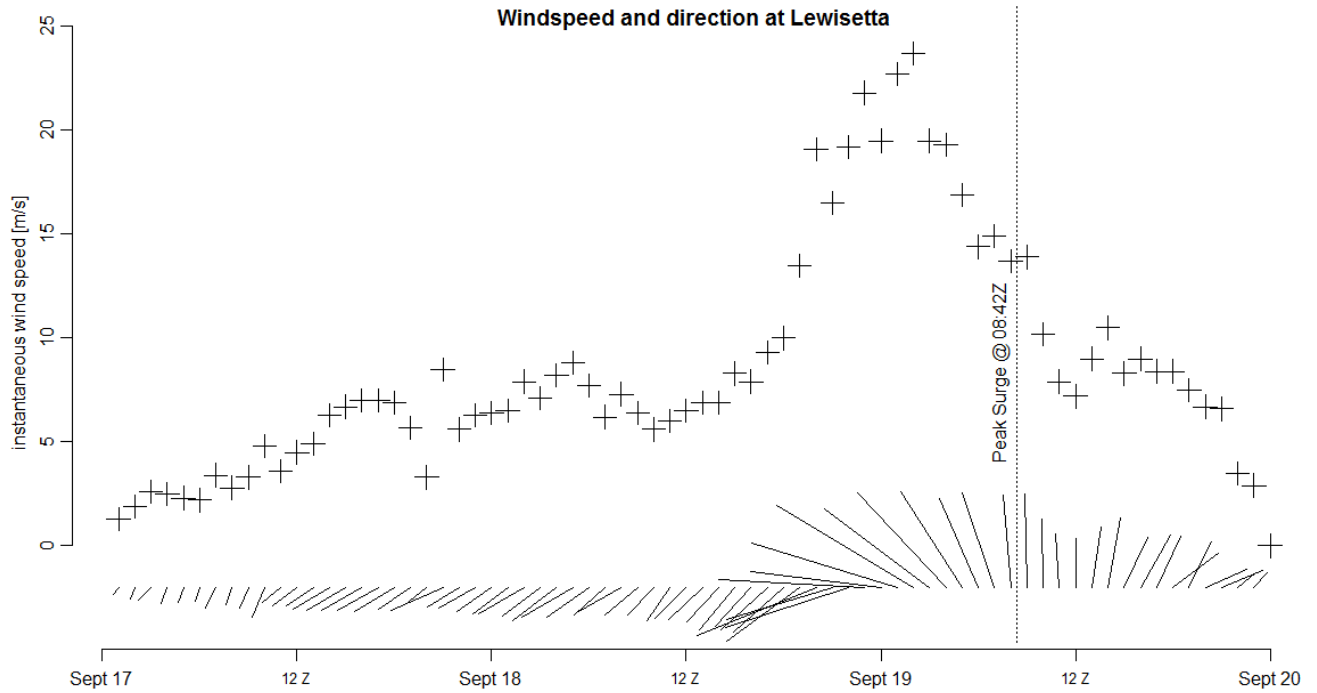
Figure 14. Observed hourly instantaneous wind direction and intensity observed at Lewisetta CO-OPS station. Vertical line indicates time of the peak surge. wind from is also shown. Stick plot on lower axis gives wind direction with base of stick along axis indicating time of observation. Note the prominent shift in direction when the eye passes the station on Sept 19 around 00Z.
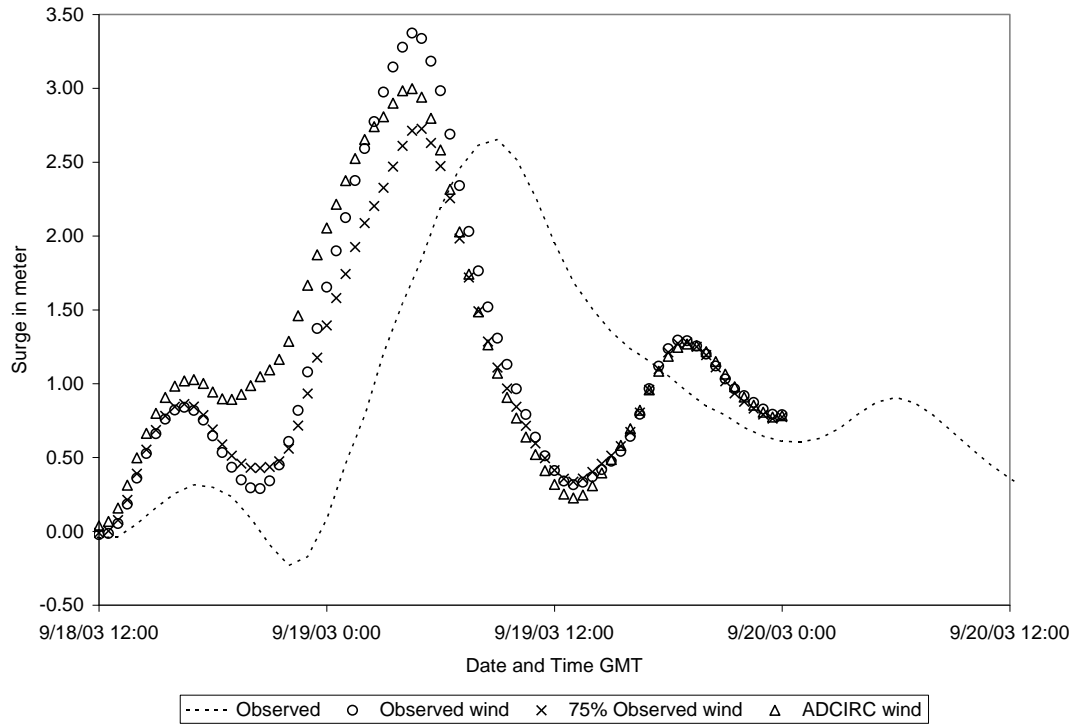
Figure 15. SOBEK simulated Hurricane Isabel surge at Washington Waterfront based on observed tidal downstream boundary conditions and three different wind forcings.